

# Adaptive Zeno measurement for qubit state preparation

Saki Tanaka\* and Naoki Yamamoto†

Department of Applied Physics and Physico-Informatics, Keio University, Yokohama 223-8522, Japan

(Dated: June 4, 2019)

This paper reconsiders the method of adaptive measurement for qubit state preparation developed by Jacobs and shows an alternative scheme that works even under unknown unitary evolution of the state. The key idea is the use of quantum Zeno effect; i.e., the measurement is adaptively changed so that the state is dynamically frozen in one of the eigenstates of the measured observable while that eigenstate approaches to the target state. Numerical simulations demonstrate that this adaptive Zeno measurement scheme offers faster and more stable convergence of the state into the target as well as higher robustness against the uncertainty of the unitary evolution, than the case of Jacobs' scheme.

PACS numbers: 03.65.Ta, 02.30.Yy, 03.67.-a

## I. INTRODUCTION

Repeated measurement of an observable that is appropriately changed according to the pre-measurement outcomes, i.e., the *adaptive measurement*, has great potential for various purposes in quantum information sciences. The first demonstration has come out in the application to quantum phase estimation [1–4]. Another application of adaptive measurement is deterministic state preparation [5–7], which all consider the case of a single qubit. A striking feature of this scheme is that a desired time evolution of the state is brought only by measurement back-action, and there is no need to introduce any external force for controlling the state.

Let us especially focus on the method developed by Jacobs [5]. This employs the schematic of a time-continuous measurement; in this case the probabilistic change of a qubit state  $\hat{\rho}$  is described by the following *stochastic master equation* (SME) [8, 9]:

$$d\hat{\rho}_t = -k_t[\hat{\sigma}_t, [\hat{\sigma}_t, \hat{\rho}_t]]dt + \sqrt{2k_t}(\hat{\sigma}_t\hat{\rho}_t + \hat{\rho}_t\hat{\sigma}_t - 2\text{Tr}(\hat{\sigma}_t\hat{\rho}_t)\hat{\rho}_t)dW_t, \quad (1)$$

where  $dW_t$  is the standard Wiener process satisfying the Ito rule  $dW_t^2 = dt$ . In the above equation,  $\hat{\sigma}_t$  and  $k_t$  represent the measured observable and the measurement strength, respectively. The adaptive measurement means that we can change  $\hat{\sigma}_t$  and  $k_t$  continuously in time, as functions of the state  $\hat{\rho}_t$ , so that  $\hat{\rho}_t$  will converge to a target state. In Jacobs' scheme, the state is assumed to be pure (this actually holds if the initial state is pure) and is thus of the form

$$\hat{\rho}_t = |\psi_t\rangle\langle\psi_t|, \quad |\psi_t\rangle = \cos(\delta_t/2)|0\rangle + \sin(\delta_t/2)|1\rangle, \quad (2)$$

where  $|0\rangle = (1, 0)^\top$  and  $|1\rangle = (0, 1)^\top$  are the target state and the initial state, respectively. Then the observable

and the measurement strength are updated according to the following laws:

$$\hat{\sigma}_t^J = \hat{\sigma}_x \sin(\delta_t) + \hat{\sigma}_z \cos(\delta_t), \quad k_t^J = \kappa\delta_t^2, \quad (3)$$

where  $\kappa$  is a positive constant. This means that the measured observable  $\hat{\sigma}_t^J$  is changed so that its eigenstates are always perpendicular to the current state  $|\psi_t\rangle$  in the Bloch sphere representation, as shown in Fig. 1. The measurement strength  $k_t^J$  is also adaptively changed, and it decreases proportionally as the state approaching to the target state; hence the measurement becomes very weak around the target. In fact, with this adaptive measurement laws (3), the time evolution of  $\delta_t \in [0, \pi]$  is given by

$$d\delta_t = \sqrt{8k_t^J}dW_t = \sqrt{8\kappa}\delta_t dW_t, \quad (4)$$

and it was numerically shown in [5] that  $\delta_t$  converges to zero as  $t \rightarrow \infty$  almost surely.

Here we come up with the question about how much the above adaptive measurement scheme is robust against certain disturbance acting on the system. Actually such robustness against a specific decohering effect was evaluated in [5]. Another specific but important disturbance is an *unknown* unitary evolution of the qubit state, in

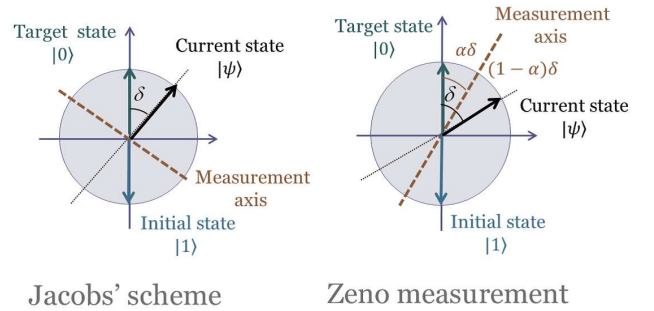


FIG. 1: (Color online) The measurement axes of Jacobs' adaptive measurement scheme (left) and the adaptive Zeno measurement scheme (right).

\*E-mail address: saki-tanaka@a6.keio.jp

†E-mail address: yamamoto@appi.keio.ac.jp

which case the driving term  $-i[\hat{H}, \hat{\rho}_t]dt$  is added to the right hand side of Eq. (1). For example, if we take a two-level atom continuously observed using the Faraday rotation technique [10] to realize the qubit system subjected to Eq. (1), such a disturbing Hamiltonian may appear and take the form  $\hat{H} = \Delta\hat{\sigma}_y$  with  $\Delta$  unknown detuning between the atomic transition frequency and the laser frequency. Note that in [5] this kind of unknown disturbance was not discussed.

In this paper, we reconsider the same control problem discussed above, yet with additional care about the influence of an unknown unitary evolution, and then propose a new adaptive measurement scheme that has clear robustness property against that disturbance. A striking feature of this scheme is in the use of *quantum Zeno effect* [11–13], which states that a repeated (or continuous in the present case) measurement freezes a quantum system in a particular state, under a unitary evolution. Therefore, it is fully expected that our adaptive measurement scheme having the Zeno effect can keep the system stable around an arbitrary target state even under influence of unknown Hamiltonian added to the system. It will be actually shown by numerical simulations that, when the state approaches to the target, the quantum Zeno effect certainly emerges, suppresses the disturbance, and stabilizes the state; as a result, our adaptive measurement scheme offers faster and more stable convergence of the state into the target as well as higher robustness against the uncertainty of the unitary evolution, than the case of Jacobs' scheme.

## II. ADAPTIVE ZENO MEASUREMENT

When we measure a system observable enough frequently, then the state is frozen in one of the eigenstates of that observable even under a certain unitary time-evolution. This is called the Zeno effect. Hence, if this measured observable is changed adaptively so that the eigenstate dragging the current state approaches into a desired target state, it is expected that the state will finally be stabilized at that target state. Based on this idea, the following observable is taken as a measured observable in Eq. (1):

$$\hat{\sigma}_t^Z = \hat{\sigma}_x \sin(\alpha\delta_t) + \hat{\sigma}_z \cos(\alpha\delta_t), \quad (5)$$

where  $\alpha \in [0, 1]$  is the parameter whose meaning is explained below. The eigenstates of the observable  $\hat{\sigma}_t^Z$  are

$$|+z\rangle = \begin{pmatrix} \cos(\alpha\delta_t/2) \\ \sin(\alpha\delta_t/2) \end{pmatrix}, \quad |-z\rangle = \begin{pmatrix} \sin(\alpha\delta_t/2) \\ -\cos(\alpha\delta_t/2) \end{pmatrix},$$

which satisfy  $\hat{\sigma}_t^Z|+z\rangle = |+z\rangle$ ,  $\hat{\sigma}_t^Z|-z\rangle = -|-z\rangle$ . In the Bloch sphere representation,  $|+z\rangle$  divides the angle between the target state  $|0\rangle$  and the current state  $|\psi_t\rangle = (\cos(\delta_t/2), \sin(\delta_t/2))^\top$  into  $\alpha : (1-\alpha)$ ; see Fig. 1. The transition probabilities of the state jumping to these eigenstates are  $p_+ = |\langle +z|\psi_t\rangle|^2 = (1 + \cos(\beta\delta_t/2))/2$  and

$p_- = |\langle -z|\psi_t\rangle|^2 = (1 - \cos(\beta\delta_t/2))/2$ , where  $\beta := 1 - \alpha$ , and they satisfy  $p_+ \geq p_-$ . This means that the state tends to move forward the direction of  $|+z\rangle$  with probability  $p_+$ . At the same time, since in this case  $\delta_t$  decreases, the eigenstate  $|+z\rangle$  moves towards the target  $|0\rangle$ . In particular, when the state reaches the target  $|0\rangle$ , or equivalently  $\delta_t \rightarrow +0$ , the eigenstate  $|+z\rangle$  also converges to the target and the transition probability  $p_+$  takes the value 1; that is, the Zeno effect emerges, and the state is frozen in the target as expected. For this reason, we call this method the *adaptive Zeno measurement* scheme or simply the Zeno measurement scheme in what follows.

Next, the measurement strength is simply set to a constant value  $k_t^Z = k^Z$ , unlike the case of Jacobs' scheme. The reason will be explained in the remark (i) given end of this section, but we here point out that this has a clear merit from a practical viewpoint. In fact, changing the measurement strength in addition to changing the measured observable definitely costs more expensive compared to the case where only the latter is required. In this sense, our scheme suited to experimental implementation.

Regarding the disturbing Hamiltonian, as discussed in Introduction, we take  $\hat{H} = \Delta\hat{\sigma}_y$ , where  $\Delta$  is an unknown constant. Note that with this Hamiltonian the state rotates around the  $y$  axis in the Bloch sphere.

Consequently, the dynamical evolution of the state under the Zeno measurement setup and the disturbing Hamiltonian introduced above is given by

$$d\hat{\rho}_t = -i\Delta[\hat{\sigma}_y, \hat{\rho}_t]dt - k^Z[\hat{\sigma}_t^Z, [\hat{\sigma}_t^Z, \hat{\rho}_t]]dt + \sqrt{2k^Z}(\hat{\sigma}_t^Z\hat{\rho}_t + \hat{\rho}_t\hat{\sigma}_t^Z - 2\text{Tr}(\hat{\sigma}_t^Z\hat{\rho}_t))dW_t. \quad (6)$$

The initial state is now on the  $x$ - $z$  plane, hence we have the dynamics of  $\delta_t$  as follows:

$$d\delta_t = 2\Delta dt - 2k^Z \sin(2\beta\delta_t)dt + \sqrt{8k^Z} \sin(\beta\delta_t)dW_t. \quad (7)$$

The linear approximated equation, which is valid when  $\delta_t \approx 0$ , is

$$d\delta_t = 2\Delta dt - 4k^Z\beta\delta_t dt + \sqrt{8k^Z}\beta\delta_t dW_t. \quad (8)$$

On the other hand, the dynamics of the same  $\delta_t$  but with Jacobs' scheme is given by

$$d\delta_t = 2\Delta dt + \sqrt{8\kappa}\delta_t dW_t. \quad (9)$$

We now compare the dynamical stabilities of the above two dynamics (8) and (9), in an intuitive way. To do this let us ignore the boundary condition  $\delta_t \in [0, \pi]$  and also set  $\Delta = 0$ ; then Eqs. (8) and (9) can be both analytically solved as follows [14]:

$$(Z) \quad \delta_t = \exp\left[(-4k^Z\beta - 4k^Z\beta^2)t + \sqrt{8k^Z}\beta W_t\right]\delta_0, \quad (10)$$

$$(J) \quad \delta_t = \exp\left[-4\kappa t + \sqrt{8\kappa}W_t\right]\delta_0, \quad (11)$$

where  $W_t = \int_0^t dW_s$ . A fair comparison of the dynamical stability of these equations can be performed by equally

setting the noise coefficient terms; i.e.,  $\sqrt{8k^Z}\beta = \sqrt{8\kappa}$ , which leads to  $k^Z\beta^2 = \kappa$ . In this case, Eq. (10) becomes

$$(Z) \quad \delta_t = \exp\left[-4\left(1 + \frac{1}{\beta}\right)\kappa t + \sqrt{8\kappa}W_t\right]\delta_0. \quad (12)$$

Equations (11) and (12) imply that, when the two adaptive measurement schemes introduce the back-action noise of the same magnitude, the Zeno measurement scheme offers the faster convergence of the state into the target of order  $e^{-4\kappa t/\beta}$ ; this term indicates no more than the emergence of the quantum Zeno effect. Of course, the above discussion makes sense only when the state is around the target. Thus we need numerical simulations to actually compare the stabilities of the two schemes, which will be discussed in the next section.

Before closing this section, we provide two remarks.

(i) Jacobs' scheme requires the adaptive tuning of the measurement strength (i.e.,  $k_t^J = \kappa\delta_t^2$  in Eq. (3)) for the dynamics of  $\delta_t$  to have the state-dependent diffusion term. As seen from the explicit solution (11), such state-dependence is indeed necessary to generate dynamical stability of  $\delta_t$ . Hence, it should be maintained that, with the Zeno measurement scheme, the diffusion term of Eq. (7) depends on the state even with the fixed measurement strength (i.e.,  $k_t^Z = k^Z$ ).

(ii) The time evolution of the fidelity between the current state  $\hat{\rho}_t$  and the target state  $|0\rangle$  is given by

$$d\langle 0|\hat{\rho}_t|0\rangle = \left[ -\Delta \sin \delta_t + k^Z \left( \cos(2\alpha\delta_t - \delta_t) - \cos \delta_t \right) \right] dt - \sqrt{2k^Z} \left[ \frac{3 + \cos \delta_t}{2} \cos(\alpha\delta_t - \delta_t) + \cos(\alpha\delta_t) \right] dW_t. \quad (13)$$

Hence, the optimum value of  $\alpha$  that maximizes the deterministic change per unit time of the fidelity is given by  $\alpha = 1/2$ . This value is actually taken in the simulations shown later.

### III. NUMERICAL SIMULATION

In this section, we numerically compare the performance of the Zeno measurement scheme to Jacobs' one, under the assumption that  $\Delta$  is *known*; this is a crucial assumption because we are then able to update  $\delta_t$  and as a result the adaptive measurement law (5) (or Eq. (3)) exactly by recursively solving Eq. (7) (or Eq. (9) for Jacobs' case). The parameters are taken as  $\kappa = 1$  and  $k^Z = 4$ . Also we set  $\alpha = 1 - \beta = 1/2$ , based on the fact mentioned in the remark (ii) in Sec. II. These parameters satisfy the condition for the fair comparison,  $k^Z\beta^2 = \kappa$ , which was given above Eq. (12). The disturbance strength  $\Delta$  takes several values. The initial condition is  $\delta_0 = \pi$ , as defined below Eq. (2).

Fig. 2 shows the time evolutions of the mean and the standard deviation of  $\delta_t$ , when  $\Delta = 0$ . The plots are obtained by averaging  $10^6$  sample paths. In Fig. 2 (a)

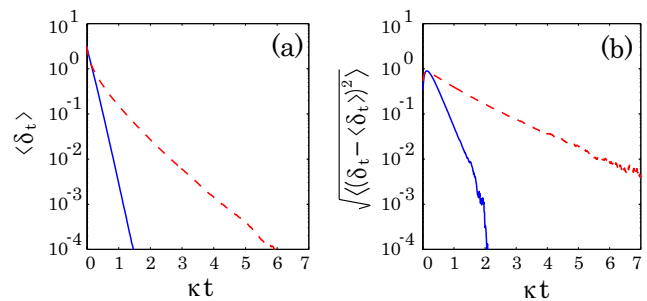


FIG. 2: (Color online) Time evolutions of (a) the mean and (b) the standard deviation of  $\delta_t$  when  $\Delta = 0$ . The solid blue and the dashed red lines correspond to the Zeno measurement and Jacobs' scheme, respectively.

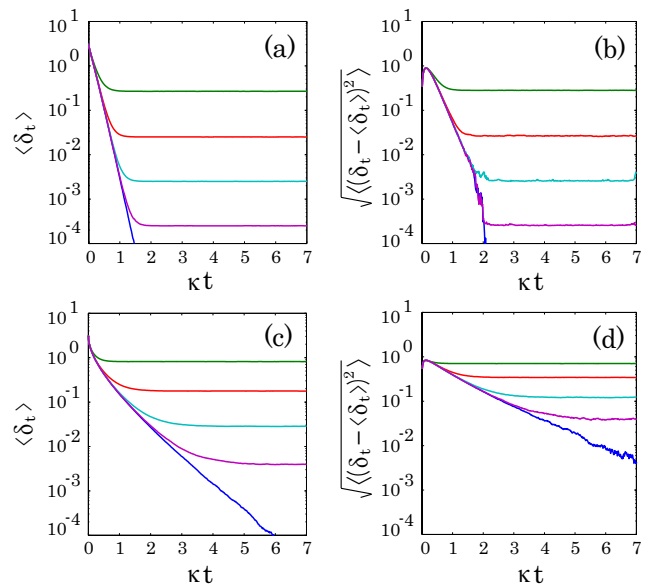


FIG. 3: (Color online) Time evolutions of (a, c) the mean and (b, d) the standard deviation of  $\delta_t$  for several values of  $\Delta$ . Figures (a) and (b) show the cases of the Zeno measurement, while Figs. (c) and (d) for the Jacobs' case. The green, red, water blue, purple, and blue lines correspond to  $\Delta = 1, 1/10, 1/10^2, 1/10^3$ , and  $\Delta = 0$ , respectively.

the solid blue and the dashed red lines correspond to the cases of the Zeno measurement and Jacobs' schemes, respectively. Both lines can be fitted by a simple function  $F(t) = C_1 e^{-C_2 t}$ ; the decay rates are obtained as  $C_2 = 10.03\kappa$  for the former case and  $C_2 = 1.357\kappa$  for the latter case (note  $\kappa = 1$  now). That is, the convergence speed in the Zeno measurement case is about 7.4 times faster in average than that in Jacobs' case. Moreover, it can be seen in Fig. 2 (b) that the state evolves with smaller fluctuation, or in other words the time-evolution of the state is more stable, when using the Zeno measurement scheme. Note that the Zeno measurement scheme was originally expected to offer faster and more stable convergence of the state to the target when  $\Delta \neq 0$ , but it is indeed the case in the ideal case  $\Delta = 0$  as well.

Next we examine several values of  $\Delta$  and show in Fig. 3 the corresponding means and standard deviations of  $\delta_t$ . Figure 3 (a, c) shows that the mean  $\langle \delta_t \rangle$  does not converge to zero when  $\Delta \neq 0$  but rather takes a constant error in the long time limit; in particular, we numerically find that this constant error is given by  $\epsilon = 0.2544\Delta\kappa$  for the Zeno measurement case (a) while in Jacobs' case (c) there is no such a simple rule. Clearly, the Zeno measurement scheme moves  $\delta_t$  towards the target  $\delta = 0$  faster with smaller constant error in average than Jacobs' case, for every values of  $\Delta$ . Similar plots are observed in Fig. 3 (b, d); that is, the state approaches to the target with smaller fluctuation, when the system is governed by the Zeno measurement scheme.

#### IV. ROBUSTNESS OF THE ADAPTIVE ZENO MEASUREMENT

Here we study the case where the external force  $\Delta$  is *unknown*. To make the situation clear, let us again consider the general SME (1) that is additionally driven by an unknown Hamiltonian  $\hat{H}$ :

$$d\hat{\rho}_t = -i[\hat{H}, \hat{\rho}_t]dt - k_t[\hat{\sigma}_t, [\hat{\sigma}_t, \hat{\rho}_t]]dt + \sqrt{2k_t}[\hat{\sigma}_t\hat{\rho}_t + \hat{\rho}_t\hat{\sigma}_t - 2\text{Tr}(\hat{\sigma}_t\hat{\rho}_t)\hat{\rho}_t]dW_t. \quad (14)$$

This *true state*  $\hat{\rho}_t$  cannot be precisely updated, due to the uncertainty of  $\hat{H}$ . Therefore, we need to devise an updating law of a *nominal state*, say  $\hat{\rho}'_t$ , only using the measurement result  $y_t$  that is subjected to the output equation

$$dy_t = \text{Tr}(\hat{\sigma}_t\hat{\rho}_t)dt + dW_t. \quad (15)$$

Note this is driven by the same  $dW_t$  as that in Eq. (14);  $dW_t$  is called the *innovation* in the framework of quantum filtering theory [15, 16]. As an updating law of  $\hat{\rho}'_t$ , we particularly use Eqs. (14) and (15) with  $\hat{\rho}_t$  and  $\hat{H}$  replaced by  $\hat{\rho}'_t$  and  $\hat{H}'$ , respectively:

$$d\hat{\rho}'_t = -i[\hat{H}', \hat{\rho}'_t]dt - k_t[\hat{\sigma}_t, [\hat{\sigma}_t, \hat{\rho}'_t]]dt + \sqrt{2k_t}[\hat{\sigma}_t\hat{\rho}'_t + \hat{\rho}'_t\hat{\sigma}_t - 2\text{Tr}(\hat{\sigma}_t\hat{\rho}'_t)\hat{\rho}'_t] \times [dy_t - \text{Tr}(\hat{\sigma}_t\hat{\rho}'_t)dt]. \quad (16)$$

Note again that  $y_t$  is the measurement result and is thus known. Hence we can recursively calculate the nominal state  $\hat{\rho}'_t$ , although it should differ from the true state  $\hat{\rho}_t$ . In particular, in the adaptive measurement setup, the observable  $\hat{\sigma}_t$  and the strength  $k_t$  are changed in time as functions of  $\hat{\rho}'_t$ .

For the specific problem under consideration, let  $\hat{H} = \Delta\hat{\sigma}_Z$  and  $\hat{H}' = \Delta'\hat{\sigma}_Z$  be the true and nominal Hamiltonians, respectively;  $\Delta$  is an unknown constant while  $\Delta'$  is a known nominal constant. Also we define  $\delta_t$  and  $\delta'_t$ , corresponding to the true and the nominal states. In the

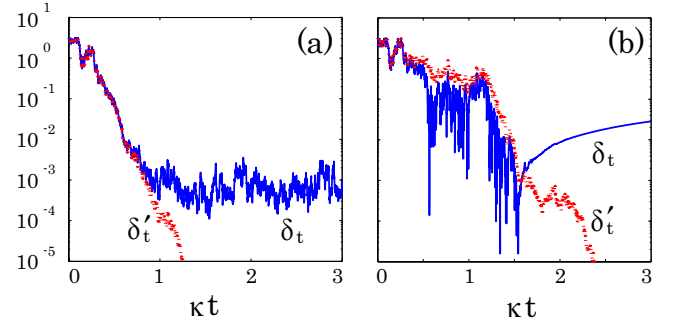


FIG. 4: Sample paths of the true variable  $\delta_t$  (solid blue lines) and the nominal one  $\delta'_t$  (dashed red lines) for (a) the Zeno measurement scheme and (b) Jacobs' scheme, where  $\Delta = 1/10^2$ ,  $\Delta' = 0$ .

Zeno measurement scheme, these variables are driven by the following equations:

$$d\delta_t = [2\Delta - 2k^Z \sin(2\delta_t - 2\alpha\delta'_t)]dt + \sqrt{8k^Z} \sin(\delta_t - \alpha\delta'_t)dW_t, \quad (17)$$

$$d\delta'_t = [2\Delta' - 2k^Z \sin(2\beta\delta'_t)]dt + \sqrt{8k^Z} \sin(\beta\delta'_t)dW_t^Z, \quad (18)$$

where

$$dW_t^Z = [\cos(\beta\delta'_t) - \cos(\delta'_t - \alpha\delta_t)]dt + dW_t.$$

Note that  $\beta = 1 - \alpha$ . The above two equations (17) and (18) take the same form when  $\Delta = \Delta'$  and  $\delta_t = \delta'_t$ . Jacobs' scheme, on the other hand, leads to the following equations to update  $\delta_t$  and  $\delta'_t$ :

$$d\delta_t = [2\Delta + 2\kappa\delta_t'^2 \sin(2\delta_t - 2\delta'_t)]dt + \sqrt{8\kappa}\delta'_t \cos(\delta_t - \delta'_t)dW_t, \quad (19)$$

$$d\delta'_t = [2\Delta' + 2\kappa\delta_t'^2 \sin(\delta'_t - \delta_t)]dt + \sqrt{8\kappa}\delta'_t dW_t^J, \quad (20)$$

where

$$dW_t^J = 2 \sin(\delta'_t - \delta_t)dt + dW_t.$$

Again, the above two equations (19) and (20) take the same form when  $\Delta = \Delta'$  and  $\delta_t = \delta'_t$ .

In Fig. 4 we show sample paths of  $\delta_t$  (solid blue line) and  $\delta'_t$  (dashed red line) for both of the adaptive measurement schemes, with the same parameters taken in Sec. III, fixed uncertainty  $\Delta = 1/10^2$ , and a typical nominal value  $\Delta' = 0$ . It is apparent from the figures that, with the Zeno measurement scheme, the true variable  $\delta_t$  is stabilized around the target  $\delta = 0$  though it still has a certain error corresponding to the constant external force, while in Jacobs' scheme  $\delta_t$  finally follows a deterministic time-evolution and goes away from zero; in every numerical simulation a similar behavior is observed.

We here address the mechanism that brings about the above drastic difference. First, since the nominal state

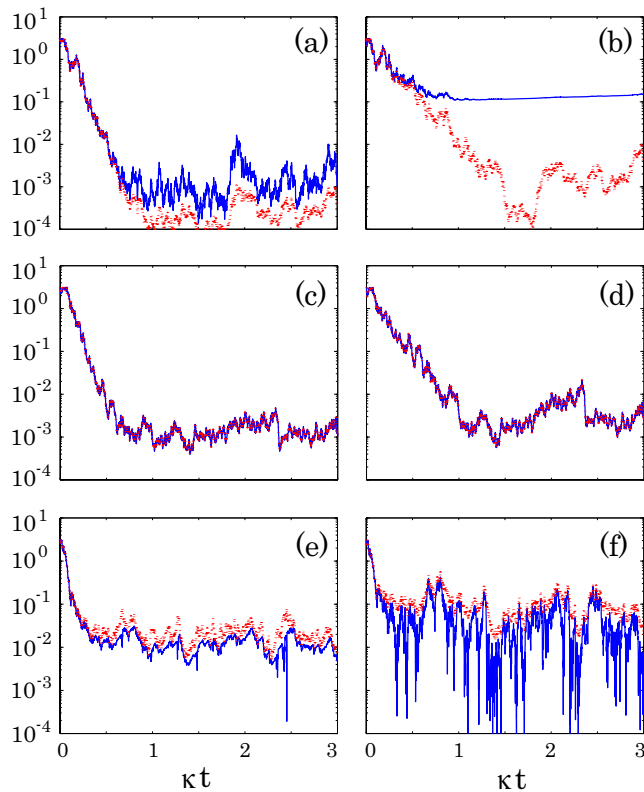


FIG. 5: Sample paths of the true variable  $\delta_t$  (solid blue lines) and the nominal one  $\delta'_t$  (dashed red lines) for (a, c, e) the Zeno measurement scheme and (b, d, f) Jacobs' scheme. For all cases, the true external force is set to  $\Delta = 1/10^2$ , while several nominal values of  $\Delta'$  are examined: (a, b) represent the case when  $\Delta' = 1/10^3$ , (c, d) for the case  $\Delta' = 1/10^2$ , and (e, f) for the case  $\Delta' = 1/10$ .

is now governed by the dynamics without uncertainty,  $\delta'_t$  converges to zero, as seen in Sec. III. When  $\delta'_t \rightarrow 0$ , the measured observable becomes  $\hat{\sigma}_t = \hat{\sigma}_z$  for both the adaptive measurement schemes, but the measurement strength becomes  $k_t^J = 0$  for Jacobs' case while  $k_t^Z = k^Z$  for the Zeno measurement case; that is, Jacobs' scheme stops to measure the system once  $\delta'_t = 0$  is reached, and consequently the true variable  $\delta_t$  turns out to follow the deterministic dynamics  $d\delta_t/dt = 2\Delta$ . In contrast, in the Zeno measurement scheme, even after  $\delta'_t$  takes zero,  $\sigma_z$  is continuously measured, implying that the true state is stabilized around the target.

The above statement holds only for the case of  $\Delta' = 0$ ; hence we take some non-zero values of  $\Delta'$  and show in

Fig. 5 the trajectories of  $\delta_t$  and  $\delta'_t$ . If  $\Delta'$  is not zero but smaller than the true value  $\Delta$  (Figs. (a, b)), we observe similar trajectories to the case of  $\Delta' = 0$ ; that is, in Jacobs' case the true variable again goes away from zero deterministically, due to the same reason stated above. In Figs. (c, d) where  $\Delta = \Delta'$ , the nominal variable  $\delta'_t$  exactly tracks  $\delta_t$ , which is the property the nominal updating laws (18) and (20) should have. Lastly, if  $\Delta'$  is bigger than  $\Delta$  (Figs. (e, f)), or in other words if we take a conservative approach for estimating  $\delta_t$ , Jacobs' scheme can stabilize the state around the target although it has a big fluctuation, while the Zeno measurement moves the state more close towards zero with much smaller estimation error.

Summarizing, in the numerical simulations shown here, the Zeno measurement scheme always offers smaller estimation error between  $\delta_t$  and  $\delta'_t$ . That is, it is fairly robust against the uncertainty of the Hamiltonian. This nice property should be particularly maintained, because without robustness the stabilization can fail as seen in Figs. 4 (b) and 5 (b).

## V. CONCLUDING REMARKS

The main features of the Zeno measurement scheme are twofold; the first is that the measured observable contains an eigenstate that eventually converges to the target state, and the other is that the measurement strength does not become weakened even when the state is close to the target, which is the crucial property bringing the robustness property. As long as the above two conditions are satisfied, it is expected that the Zeno measurement scheme can be generalized to the multi-dimensional case. However, in many situations any physically available observable does not contain an eigenvector that is identical to a desired target state, and then the Zeno measurement scheme cannot be used in order to prepare that target state. Rather, as discussed in [6, 7], in such a case, a certain weak measurement may work for generating a target state. But a critical requirement for this measurement is that the measurement strength should be weakened when the state approaches to the target; then, the system can become fragile against unknown disturbance, as seen in Sec. IV. Exploring an adaptive measurement method that overcomes this issue is an interesting future work.

We thank Yuzuru Kato for his contribution to have the remark (ii) in Sec. II.

[1] H. M. Wiseman, Phys. Rev. Lett. **75**, 4587 (1995); H. M. Wiseman and R. B. Killip, Phys. Rev. A **56**, 944 (1997); H. M. Wiseman and R. B. Killip, Phys. Rev. A **57**, 2169 (1998); D.W. Berry and H. M. Wiseman, Phys. Rev. Lett. **85**, 5098 (2000); D.W. Berry and H. M. Wiseman, Phys.

Rev. A **65**, 043803 (2002).

[2] M. A. Armen et al., Phys. Rev. Lett. **89**, 133602 (2002).

[3] M. Tsang, J. H. Shapiro, and S. Lloyd, Phys. Rev. A **79**, 053843 (2009).

[4] T. A. Wheatley, et. al. Phys. Rev. Lett. **104**, 093601

- (2010).
- [5] K. Jacobs, *New J. Phys.* **12**, 043005, (2010).
  - [6] S. Ashhab and F. Nori, *Phys. Rev. A* , **82**, 06103 (2010).
  - [7] H. M. Wiseman, *Nature* **470**, 178 (2011).
  - [8] R. Van Handel, J. K. Stockton, and H. Mabuchi, *IEEE Trans. Automat. Contr.* **50**, 768/780 (2005).
  - [9] H. M. Wiseman and G. J. Milburn, *Quantum measurement and Control* (New York, Cambridge University Press, 2010).
  - [10] J. K. Stockton, *Continuous Quantum Measurement of Cold Alkali-Atom Spins*, Ph.D Thesis, California Institute of Technology, 2006.
  - [11] B. Misra and E. C. G. Sudarshan, *J. Math. Phys.* **18**, 756 (1977).
  - [12] P. Facchi, H. Nakazato, and S. Pascazio, *Phys. Rev. Lett.* **86**, 2699 (2001).
  - [13] Y. Matsuzaki, S. Saito, K. Kakuyanagi, and K. Semba, *Phys. Rev. B* **82**, 180518(R) (2010).
  - [14] B. Oksendal, *Stochastic Differential Equations; An Introduction with Applications* (Berlin, Springer, 2003).
  - [15] V. P. Belavkin, *J. Multivariate Anal.* **42**, 171/201 (1992).
  - [16] L. Bouten, R. van Handel, and M. R. James, *SIAM J. Control Optim.* **46**, 2199/2241 (2007).